IJCSE International Journal of Computer Sciences and Engineering Open Access
Research Paper Vol.-7, Special Issue-18, May 2019 E-ISSN: 2347-2693

Cost Effective Rotary to Linear Motion Conversion for a Near Omni-Directional Robotic Vehicle

H. Masum

Dept. of Mechanical Engineering, Ghani Khan Choudhury Institute of Engineering and Technology (GKCIET), Malda, West Bengal, India

Corresponding Author: kingmasum@gmail.com, Tel.: +91-8910831384

Available online at: www.ijcseonline.org

***Abstract*—**The near omni-directional hexapod vehicle is an autonomous robotic kit which can move in three-dimensional space. It is able to rotate any angle at its any state of movement without compromising its speed. Rotary-to-linear motion conversion is concerned with taking the rotational motion and torque from an actuator and producing a linear motion and force on the output. In this paper, an effort has been made to design the mechanical system of a robotic vehicle having six legs which can serve as a compliant mobile platform. The design has been validated through simulation. It has a limited number of degree-of-freedom to minimize the mechanical motion constraints as well as lower power consumption. The hexapod design of the vehicle offers great static stability during walking.

***Keywords*—** Hexapod vehicle, Omni-directional robotic kit, Pantograph leg, Stability margin

I. INTRODUCTION

Robotic vehicle is a moving machine which is able to execute autonomous movements and functions automatically upto a great extent. Majority of robots today are used to do precision work, repetitive actions or jobs considered too dangerous for humans.

Although the concept of robotics has originated in the ancient world, the first robot was created in 250 B.C. as a water clock by a Greek physicist and inventor, Ctesibius of Alexandria [1]. The modernization in this field has noticed with the initiation of the Industrial Revolution to allow application of complex mechanics and subsequent innovation of electricity. The remote control vehicles were introduced in the 1890's by Nikola Tesla [2]. G.E. Quadruped was built in 1968 by General Electronics Corporation which is considered as the first manually vehicle to demonstrate good terrain adaptability and obstacle avoidance capability [3]. Each leg possessed three degrees of freedom (DoF). This 12-DoF manual controlled system was complex in operation and thus emphasized the need of computer-controlled systems for the multi degree of freedom vehicles. The first successful use of digital computer was in the 1970s by Robert McGhee's group [4]. They developed an insect-inspired walking machine called OSU Hexapod that could walk with a number of standard gaits, turn and avoid obstacles. PV-II was built by Hirose et al in 1980 at Tokyo of Technology, Japan [5]. Earlier they developed a four-legged walking machine called KUMO-I which had an individual driving motor and clutch on each leg to generate the variable walking motion. PV-II was the first stair-climbing robot based on sensory motion control [6]. Collie is a quadruped walking machine robot with three DOF per leg, which was developed to accomplish both static and dynamic walking. In 1994, C.M.U. developed DANTE II. It was an aluminum body consisting of eight legs, four of which were always on the ground [7]. It was deployed in the active crater of Alaskan volcano, on a five day mission to take samples and gather data on volcano activity. Titan series of robots were developed at Tokyo Institute of Technology [8]. They all had four legs. Titan III consisted pantograph leg was developed for the sake of realization of higher terrain adaptability. Titan VI was developed to test the dynamic motion of the robot in climbing up and down the stairs. Titan VII was designed to use as a scaffold to assist civil works carried out at steep slope. Artificial intelligence has been integrated into digitally controlled industrial robots since the twentieth century. Legged robots have advantages over wheeled or tracked vehicles that it can move over rough and discontinuous terrain with more agility. The walking robots with at least 3-DoF on each leg are capable of strafing movements such as crabbing, however, 1-DoF and 2-DoF legs can only move in one and two dimensions, respectively. These make the system more complex, heavy in weight and extra power required. Therefore, the design of a near omni-directional robotic vehicle with 2-DoF per leg and 1-DoF at the center of the body is proposed here which will be capable to move in

three-dimensional space. The mechanism minimizes mechanical motion constraints with great static stability as well as lowering power consumption. The design of the robotic vehicle initiated with envisage of targeted design parameters, then kinematics and estimation of different force acting on it, development of CAD models, simulation, verifying stability margin, and then a conclusion.

II. METHODOLOGY

Study of various walking robot [5]-[12] suggests few essential salient features as follows, which have targeted through design parameter for effective working of the vehicle in vast type of terrain:

- Ability to move the vehicle at varying velocities as required.
- Offer stable robot platform
- It would eliminate the dynamic reasons for poor energy efficiency
- Minimizes number of DoF to walk at regular terrain

In view of the targeted design parameters, the design has been initiated with the consideration that the length of the vehicle stride will be 200 mm and speed of the vehicle will 0.75 m/min. Figure 1 represents the workflow of the design of an omni-directional robotic vehicle:

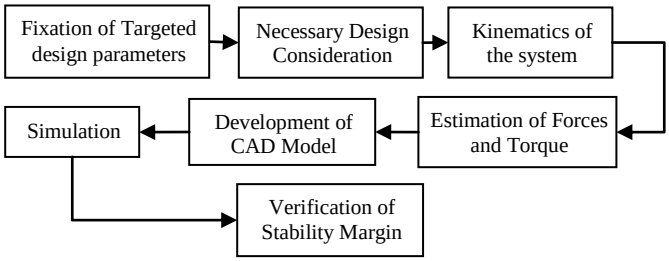

Figure 1. Workflow for design of the robotic vehicle

III. DETAIL DESIGN OF THE MECHANICAL SYSTEM

The mechanical system of the vehicle is modeled as a kinematic chain with several rigid links of legs and two base frames connected in series and parallel by either revolute or prismatic joints driven by servo motors. The design of the walking robot consists of two sets of three legs attached with two body halves (base frames) jointed revolving joint. When the legs of a base frame are on the ground (support phase), actuators give a backward linear displacement to the foot with respect to the vehicle body. Since the foot kept on the ground, it propels the robot body in forward direction. At the same time, the legs on another base frame are lifted in the air (transfer phase) and move backward to its forward position. After completion of transfer phase the legs are shifted to support phase and the legs on the support phase shifts to the transfer phase. With the repetitions of those two phases by the two set of legs, a continuous movement can achieve. During a change in direction of movement of the vehicle, the connecting actuator of two base frames gives a required rotation to the body half (base frame) on the transfer phase. Hence, the legs on the transfer phase touch the ground at new (desired) direction and continue their move further on latest direction until further change in direction is required.

The hexapod model consists of inverted pantograph legs having two translational DoF on the leg plane. Two dimensional pantograph legs were chosen because of its controllability and energy efficiency [4][10]. Additional DoF at leg would have been redundant for basic walking and would have required a greater amount of complexity, power and processing to control [13]. Another rotational DoF provided at vehicle's body centre about the vertical axis for turning. The pantograph legs have unique design having enough flexibility to ensure efficient obstacle avoiding approach and effective postural control. The legs consist of a rotational joint for forward progression and a prismatic joint for rising as shown in Figure 2.

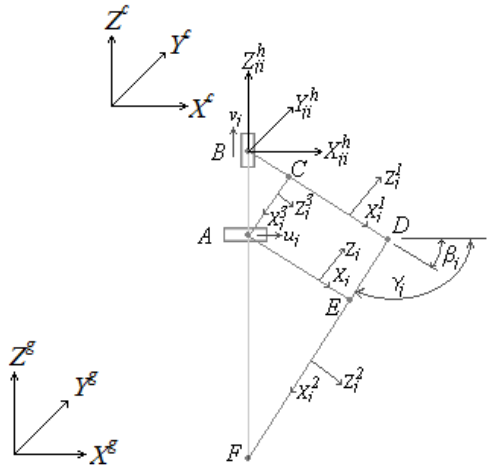

Figure 2. Pantograph leg with co-ordinate system

The motion of each link of legs can be expressed with reference to the centre of mass (CoM) of the vehicle as well as with the fixed coordinate system of ground's. The fixed coordinate system of ground has designated as (X^g, Y^g, Z^g) and is fixed with the working terrain while coordinate system fixed with the vehicle's CoM is (X^c, Y^c, Z^c). Therefore, the vehicles coordinate system with reference to the ground coordinate system is expressed by the translation matrix and a rotational matrix as follows:

$$T_{xyz} = \begin{bmatrix} 1 & 0 & 0 & X \\ 0 & 1 & 0 & Y \\ 0 & 0 & 1 & Z \\ 0 & 0 & 0 & 1 \end{bmatrix} \quad \text{and} \quad R_{z,\psi} = \begin{bmatrix} \cos\psi & -\sin\psi & 0 & 0 \\ \sin\psi & \cos\psi & 0 & 0 \\ 0 & 0 & 1 & 0 \\ 0 & 0 & 0 & 1 \end{bmatrix} \quad ..(1)$$

where, Ψ = Heading

The progressed coordinate of a leg (X^h_{ji}, Y^h_{ji}, Z^h_{ji}) attached to the body at the hip joint of the leg 'j' at the plate 'i' after a progression of 'x' in X-direction and an amount 'y' in Y-direction is

$$ {}^eP^b = T_{XYZ}.R_{Z,\Psi}.T_{xy}.{}^bT^h{}_{ji}.{}^hP^f_{ji} $$

$$ = \begin{bmatrix} 1 & 0 & 0 & X \\ 0 & 1 & 0 & Y \\ 0 & 0 & 1 & Z \\ 0 & 0 & 0 & 1 \end{bmatrix} \begin{bmatrix} \cos\Psi & -\sin\Psi & 0 & 0 \\ \sin\Psi & \cos\Psi & 0 & 0 \\ 0 & 0 & 1 & 0 \\ 0 & 0 & 0 & 1 \end{bmatrix} \begin{bmatrix} 1 & 0 & 0 & \sqrt{(x^2+y^2)} \\ 0 & 1 & 0 & 0 \\ 0 & 0 & 1 & 0 \\ 0 & 0 & 0 & 10 \end{bmatrix} . {}^bT^h_{j,i} \begin{bmatrix} (1+R)u_j \\ 0 \\ -\left(Z^h_{fji}+e\right) \\ \hline R \\ 1 \end{bmatrix} $$

……(2)

where, ${}^bT^h_{j,i}$ is the translational matrix.

Figure 2 shows that 'u' is the translational driving axis in the horizontal direction and 'v' is the translational driving axis in the vertical direction. Therefore, the forward kinematic correlates the foot position (${}^hX^f_{ji}$, ${}^hY^f_{ji}$, ${}^hZ^f_{ji}$) with the displacement of the two actuators (u_j , v_j) is

$$ {}^hP^f_{ji} = [\,{}^hX^f_{ji}, {}^hY^f_{ji}, {}^hZ^f_{ji}\,]^T = \begin{bmatrix} (1+R)u_j \\ 0 \\ -(e+Rv_j) \end{bmatrix} \quad .. (3) $$

where R is a constant represents the magnification factor of movement which is the ratio of AF and AB and *e* is the distance *u*-axis offsite from X^l_j axis in the mounting plane

and the inverse kinematics is $W_j = \begin{bmatrix} \frac{X^h_{fji}}{(1+R)} \\ \frac{-\left(Z^h_{fji}+e\right)}{R} \end{bmatrix}$ .. (4)

The velocity and acceleration of the above equation obtained by taking the first and second derivatives of the inverse position equations respectively, as

$$ \dot{W}_j = J_j^{-1}.{}^h\dot{P}^f_{ji} \quad \text{and} \quad \ddot{W}_j = J_j^{-1}\left[{}^h\ddot{P}^f_{ji} - V_{aj}\right] \quad .. (5) $$

The optimization of different links of the leg has been done applying Chebyshev's accuracy point method. As shown in Figure 3, the accuracy points according to Chebyshev's spacing are given by

$$ Z_l = a + h.\cos\frac{[(2l-1).180]}{2k} \quad .. (6) $$

where k = number of nodal points and l = nodal points 1, 2, 3…

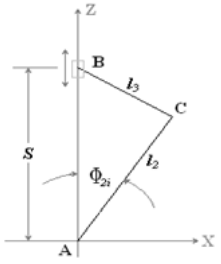

Figure 3. Free-body diagram of Slider-link mechanism

According to design criteria, few parameters have been fixed and these are the vertical input stroke at the point B is = 30 mm, the initial sliding point, S_f = 20 mm, number of nodal point, k=3 and the initial sliding angle, Φ_{2i} = 29° as the range of sliding angle should be within 45° to 22° out of which it will introduce a sliding motion constraints. Therefore, final or extreme point is, S_i = (20+30) = 50 and the final sliding angle, Φ_{2f} = 44°.

Then, $C = \frac{(S_f - S_i)}{(\Phi_{2f} - \Phi_{2i})^2} = 0.0814$; $a = \frac{(z_i + z_f)}{2} = 35mm$ and

$h = \frac{(z_i - z_f)}{2} = 15mm$ .. (7)

Therefore, z_1 = 47.99 mm, z_2 = (35+15.cos 90°) = 35 mm & z_3 = (35+15.cos 150°) = 22.01 mm .. (8)

Again, $r_x = \frac{(\Phi_{2f} - \Phi_{2i})}{(z_f - z_i)} = 0.64$ .. (9)

From the Eq. (9), it can be written as $\frac{(\Phi_{2l} - \Phi_{2i})}{(z_l - z_f)} = r_x$ ..(10)

Consequently, $^{\Phi_{21}}$ = 45.214°, $^{\Phi_{22}}$ = 36.9° & $^{\Phi_{23}}$ = 28.586° ..(11)

From the Eq. (7), it also can be written as $S_l = S_i + C(\Phi_{2l} - \Phi_{2i})^2$ .. (12)

and S_1 = 23.885 mm, S_2 = 42.5 mm and S_3 = 49.796 m ..(13)

From the four bar link mechanism,

$$ AC^2 = l_3^2 = (z_A - z_B)^2 + (x_A - x_B)^2 $$
$$ = (l_2\cos\Phi_{2i} - S_l)^2 - (l_2\sin\Phi_{2l} - S_l)^2 $$

$$ \therefore \quad S_l^2 = 2.l_2.S_l.\cos\Phi_{2i} - l_2^2 + l_3^2 = k_1.S_l.\cos\Phi_{2i} - k_2 \quad ..(14) $$

where, $k_1 = 2.l_2$ and $k_2 = l_2^2 - l_3^2$

After substituting related points in the Eq. (14), the following equation obtained $16.826k_1 - k_2 = 570.493$ and $33.987k_1 - k_2 = 1889.25$ .. (15)

By equating the above two equations, k_1 =72.01 & k_2 =641.14

Then, the l_2 = 36 mm & l_3 = 25.6 mm.

If the *magnification factor* of movement, *R*, is 4 then L, then the leg links lengths are, L_1 = 128 mm, L_2 = 180 mm, L_3 = 36 mm and L_4 = 102.4 mm.

Figure 4 represents the free body diagram of different moving links of the pantograph leg mechanism.

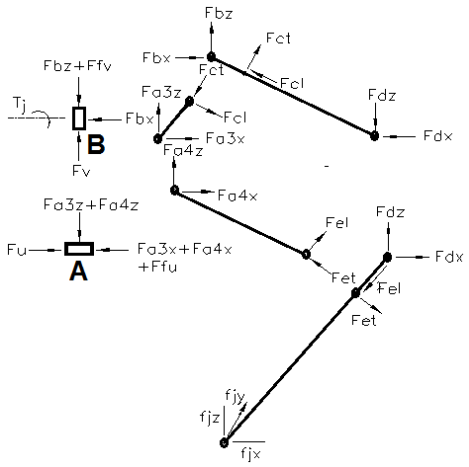

Figure 4. Free-body diagram of pantograph leg

The forces acting on different the reciprocating joints can be determined considering the system at static equilibrium. For example, the horizontal components of reaction force acting at foot is

$$F_{jx} = -F_{dx} - F_{et}.\sin\gamma - F_{el}.\cos\gamma \quad .. (16)$$

and the vertical components of reaction force acting at foot is

$$F_{jz} = F_{el}.\sin\gamma - F_{dz} - F_{et}.\cos\gamma - m_{l2}.g_{jz} \quad .. (17)$$

where, F_{ix} & F_{iz} are the horizontal and vertical components reaction force of the j^{th} foot.

From the diagram shown in Figure 4, it can be written that the resultant force at joint A which acts horizontally,

$$F_A = \sqrt{(F_{a3x} + F_{a4x})^2 + (F_{a3z} + F_{a4z})^2} \quad ..(18)$$

Resultant force at joint B which acts vertically,

$$F_B = \sqrt{(F_{bx})^2 + (F_{bz})^2} \quad ..(19)$$

and the torque, $$T = \frac{L.F}{\sqrt{n^2 - \sin^2\theta}} \quad .. (20)$$

where, L = length of connecting rod, and n = L/r i.e., the ratio of connecting rod length to crank length.

For the body central servo, torque is $T_c = Mc.g.r_m$ ..(21)

where, M_c = mass of body and three legs = M_b+3 M_l, g = gravitational acceleration and r_c = radius of motor shaft

With the evaluation of mass of different components the estimated torque (max.) is 0.3353 N-m. Accordingly, HSR-5995TG digital servo motor of rating torque = 24.0 kg-cm (2.3544 N-m) has been chosen. A prototype has been developed in CAD environment to validate desired functions of vehicle as shown in Figure 5.

Figure 5. CAD model of the prototype

IV. RESULTS AND DISCUSSION

For detail motion analysis of the vehicle, different nature of terrain and different obstacle are considered to get desired movement in a dynamic simulator. At the end of analysis, the system has been simulated with MATLAB Sim-mechanics platform to verify the kinetic behavior. Figure 6 shows different movement of omni-directional vehicle in a dynamic simulation platform.

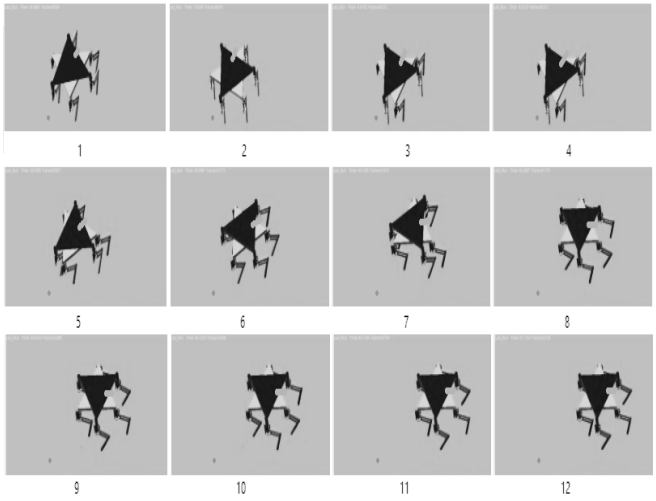

Figure 6. Movement of omni-directional vehicle in a dynamic simulation platform

Any moving system is called statically stable when the CoM falls within the support polygon. The stability margin refers a minimum projected distance of the CoM of the entire system with the support polygon confined by the foot points on the ground at rest. For quantification, the stability margin has been evaluated. A code has been generated in MATlab for evaluation of stability margin at various locations during motion. Figure 7 shows the stability margin of the system from where it is observed that the minimum margin exist at the end of first half cycle which is greater than zero and maximum margin reaches at the moment when the all six legs ground during of phase change of legs. Therefore, the system is completely static stable.

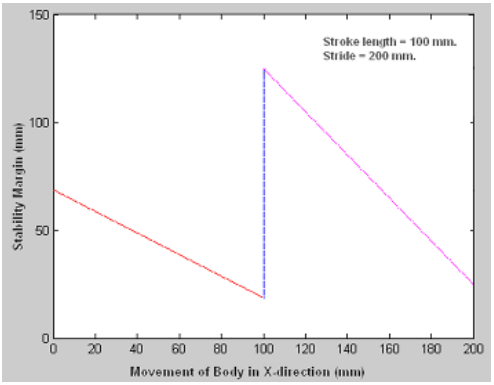

Figure 7. Variation of Stability margin with body movement

V. CONCLUSION AND FUTURE SCOPE

The design of a near omni-directional legged vehicle is proposed here that can rotate in any direction when it is moving up to 180° in both sides. It offers uniform motion with minimized the mechanical motion constraints by limiting number of DoF. The stability margin of this hexapod vehicle varies from 125 mm to 18.75 mm which makes the vehicle highly static stable. Further the mammal type of legs minimizes the power consumption. The above work primarily explores the mechanics, kinematics and dynamics of a near omni-directional vehicle having six legs. However, further effort can be made on electronics part, control and detail motion planning of the vehicle.

REFERENCES

[1] K. P. Valavanis, G. J. Vachtsevanos, P. J. Antsaklis, "*Technology and Autonomous Mechanisms in the Mediterranean: From Ancient Greece to Byzantium*", Proceedings of the European Control Conference, **Greece**, pp.**263-270**, **2007**.

[2] J. W. Simatupang, M. Yosua, "*Remote Controlled Car using Wireless Technology*", Journal of Electrical and Electronics Engineering, Vol.**1**, No.**2**, pp.**56-61**, **2016**.

[3] J. A. T. Machado, M. F. Silva, "*An overview of Legged Robots*", Conference: MME 2006–International Symposium on Mathematical Methods in Engineering, **Turkey**, **2006**.

[4] K. J. Waldron, R. B. McGhee, "*The Mechanics of Mobile Robots*", Robotics, Vol.**2**, No.**2**, pp.**113-121**, **1986**.

[5] S, Hirose, Y, Fukuda, K. Yoneda, A. Nagakubo, H. Tsukagoshi, K. Arikawa, G. Endo, T. Doi, R. Hodoshima, "*Quadruped Walking Robots at Tokyo Institute of Technology Design, Analysis, and Gait Control Methods*", IEEE Robotics & Automation Magazine, vol.**16**, No.**2**, pp.**104-114**, **2009**.

[6] U. Saranli, M. Buehler, D. E. Koditschek, "*RHex: A Simple and Highly Mobile Hexapod Robot*", The International Journal of Robotics Research, Vol.**20**, No.**7**, pp. **616-631**, **2001**.

[7] N. Koyachi, H. Adachi, M. Izumi, T. Hirose, N. Senjo, R. Murata, T. Arai "*Control of Walk and Manipulation by A Hexapod with Integrated Limb Mechanism: MELMXNTIS-1*", Proceedings of the 2002 IEEE International Conference on Robotics & Automation, **Washington**, pp.**3553-3558**, **2002**.

[8] A. M. Hoover, E. Steltz, R. S. Fearing, "*RoACH: An autonomous 2.4g crawling hexapod robot*", IEEE/RSJ International Conference on Intelligent Robots and Systems, **France**, pp.**26-33**, **2008**.

[9] M. H. Raibert, "*Legged Robots*", Communications of the ACM, Vol. **29**,No.**6**, pp.**499-514**,**1986**.

[10] F. Delcomyn, M. E. Nelson, "*Architectures for a biomimetic hexapod robot*", Robotics and Autonomous Systems, Vol.**30**, pp. **5–15**, **2000**.

[11] W.A. Lewinger, M.S. Branicky, R.D. Quinn, "*Insect-inspired, Actively Compliant Hexapod Capable of Object Manipulation*", Climbing and Walking Robots. Springer, **Berlin**, **Heidelberg**, pp.**65-72**, **2006**.

[12] M. O. Sorin, M. Niţulescu, "*Hexapod Robot. Virtual Models for Preliminary Studies*", 15th International Conference on System Theory, Control and Computing, **Sinaia**, pp.**1-6**, **2011**.

[13] G Jianhua, "*Design and Kinematic Simulation for Six-DOF Leg Mechanism of Hexapod Robot*" Proceedings of the IEEE International Conference on Robotics and Biomimetics, **China**, pp.**625-629**, **2006**.

Authors Profile

H Masum received the B.E. degree in Mechanical Engineering from VTU, Belgaum, India in 2005 and M.Tech. degree in Production & Design Engineering under Mechanical Engineering from NIT, Durgapur, WB, India in 2007. During 2007-2013, he worked as Sr. Engineer in M.N. Dastur & Co. (P.) Ltd., Kolkata, India, to design various units of steel plants, power plants and ferro-alloy plants for many nations. He has submitted his Ph.D. thesis entitled "Intelligent Active Ankle Foot Prosthesis Using Multisensory Feedback" in October 2018 at Indian Institute of Engineering Science and Technology (IIEST), Shibpur, Howrah, India. He is also with Ghani Khan Choudhury Institute of Engineering and Technology, Malda (a Centrally Funded Technical Institute under Ministry of HRD, Govt. of India) as Assistant Professor and Head, Dept. of Mechanical Engineering.

